ULTRASONIC IMAGING **32,** 131- 142 (2010)

# Quantitative Ultrasound Assessment of Cervical Microstructure

HELEN FELTOVICH,[1,2] KIBO NAM[1] AND TIMOTHY J. HALL[1]

[1]*Department of Medical Physics*
*1111 Highland Ave.*
*University of Wisconsin, Madison, WI 53703*
*hfeltovich@gmail.com*

[2]*Department of Obstetrics and Gynecology*
*1 South Park*
*University of Wisconsin*
*Madison, WI, 53711*

The objective of this preliminary study was to determine whether quantitative ultrasound (QUS) can provide insight into, and characterization of, uterine cervical microstructure. Throughout pregnancy, cervical collagen reorganizes (from aligned and anisotropic to disorganized and isotropic) as the cervix changes in preparation for delivery. Premature changes in collagen are associated with premature birth in mammals. Because QUS is able to detect structural anisotropy/isotropy, we hypothesized that it may provide a means of noninvasively assessing cervical microstructure. Thorough study of cervical microstructure has been limited by lack of technology to detect small changes in collagen organization, which has in turn limited our ability to detect abnormal and/or premature changes in collagen that may lead to preterm birth. In order to determine whether QUS may be useful for detection of cervical microstructure, radiofrequency (rf) echo data were acquired from the cervices of human hysterectomy specimens ($n$ = 10). The angle between the acoustic beam and tissue was used to assess anisotropic acoustic propagation by control of transmit/receive angles from –20° to +20°. The power spectrum of the echo signals from within a region of interest was computed in order to investigate the microstructure of the tissue. An identical analysis was performed on a homogeneous phantom with spherical scatterers for system calibration. Power spectra of backscattered rf from the cervix were 6 dB higher for normal (0°) than steered (±20°) beams. The spectral power for steered beams decreased monotonically (0.4 dB at +5° to 3.6 dB at +20°). The excess difference (compared to similar analysis for the phantom) in normally-incident (0°) versus steered beams is consistent with scattering from an aligned component of the cervical microstructure. Therefore, QUS appears to reliably identify an aligned component of cervical microstructure; because collagen is ubiquitously and abundantly present in the cervix, this is the most likely candidate. Detection of changes in cervical collagen and microstructure may provide information about normal versus abnormal cervical change and thus guide development of earlier, more specific interventions for preterm birth.

KEY WORDS: Cervical assessment; cervical insufficiency; cervical microstructure; cervical ultrasound, preterm delivery.

## INTRODUCTION

The pregnant cervix is unique in that its functions are diametrically opposed: its job is to remain closed until the fetus is fully developed and then to open entirely for delivery. Failure of these mechanisms causes morbidity across a spectrum from preterm births to postterm pregnancies. The ramifications of preterm birth are particularly staggering. In the US, 1 of every 8 births is preterm; prematurity is responsible for 20% of mental retardation, 30% of vision impairment and 50% of cerebral palsy.[1, 2] Long-term effects include cardiovascular disease, hypertension, diabetes, dyslipidemia, neurocognitive disorders, respiratory conditions and cancer.[1,2]



0161-7346/10 $18.00

The spontaneous preterm birth rate for singletons has not changed in more than a century. Drugs that treat infection, reduce inflammation and/or inhibit uterine contractions are ineffective and bedrest and/or cervical cerclage (a stitch around the cervix) show little if any benefit in randomized-controlled trials.[1-3] Progesterone has recently shown promise but its dosage, administration and, especially, its mechanism remain to be elucidated.[4-8]

Risk assessment has improved through ultrasound monitoring of cervical length and fetal fibronectin assessment.[9] Unfortunately, the utility of these tests is limited; in the words of the American College of Obstetricians and Gynecologists, their strength ''may rest primarily with their negative predictive value given the lack of proven treatment options to prevent preterm birth''[10] Given a problem this compelling, the current lack of solutions may seem surprising. In a recent review, Romero et al remark that ''this area of clinical investigation has been overlooked.''[3]

More likely, the obstacle is related to the difficulties inherent in objectively assessing microstructural cervical change. Collagen, the most ubiquitous component of the cervical microstructure (makes up 85%), is aligned and organized in the nonpregnant cervix and becomes progressively disorganized as the cervix remodels throughout pregnancy in preparation for delivery.[11-17] The first month of pregnancy initiates a slow, progressive phase of collagen reorganization.[14, 15] Near delivery, a second phase involves rapid and marked reorganization of the microstructure, causing macrostructural changes (including cervical shortening).[16, 17] The third phase is active dilation during labor and the fourth is recovery of the microstructure. [16, 17] The reoganizational phases are essential; uterine contractions in the absence of cervical remodeling changes do not effect delivery.[18] However, premature disorganization (demonstrated by increased extractability of collagen) is correlated to a history of preterm birth in women.[14]

Clearly, thorough comprehension of cervical remodeling in pregnancy is critical to understanding preterm birth. Unfortunately, the specific biomechanics and biochemistry of this process remains poorly understood. One preterm birth investigator summarized the issue nicely: "Mechanisms are not well described. At present in clinical routine there is no reliable, objective, and quantitative method to monitor early cervical changes includ[ing] detection of ripening leading to cervical incompetence and eventual preterm birth."[11]

Inherent in this statement is the recognition that a more comprehensive understanding of these processes should lead to more appropriate interventions. In other words, our incomplete understanding of cervical structure and function limits our ability to conceive of novel therapeutic or preventive approaches. Therefore, assessing cervical change seems paramount to understanding the mechanisms related to preterm birth. Finding a noninvasive, objective way to examine cervical microstructure has been exceedingly difficult, however. The primary cervical assessment tool (Bishop score) is subjective, relying on digital evaluation of cervical softness, dilation and length[19] and provides no means of understanding the processes leading to birth: the factors and pathways involved in the microstructural arrangements that cause cervical change.

Some microscopy techniques are useful for exploring cervical microstructure where tissue biopsies are possible. Polarized light microscopy distinguishes anisotropic from isotropic tissues because the former are more birefringent (due to unequal splitting of the light wave). An unremodeled cervix should be more birefringent than the remodeled and it is; the pregnant rat's cervix shows progressive isotropy as it softens prior to delivery.[20] Further, lesser birefringence is associated with reduced tensile strength.[21] Recently, Myers et al have developed a comprehensive biomechanical and biochemical approach to investigating the cervical extracellular matrix in the human. Their work supports that human cervical collagen (especially in the nonpregnant state) behaves anisotropically.[22]

Unfortunately, biopsy of the pregnant woman's cervix is impractical and there are currently no reliable noninvasive modalities. Quantitative ultrasound analysis of B-mode im-

ages shows a lower mean gray scale measurement in patients destined for preterm delivery, but it is imprecise .[23, 24] Decreased collagen organization (decreased crosslinking of the fibers) is associated with lesser light-induced fluorescence; fluorescence decreases progressively throughout the rat pregnancy, which correlates with reduced tensile strength.[25] In humans, fluorescence decreases as gestation progresses and, in most patients presenting for induction of labor, fluorescence decreases after administration of a cervical-ripening agent, presumably because of collagen disorganization.[25] However, the technique is difficult and cumbersome.

Measurement of ultrasonic attenuation is logical; as the cervix ripens, spacing between the fibrils increases from water and proteins and the collagen structure changes from aligned to disorganized, attenuation should change. One group measured attenuation in rat cervices throughout gestation, but did not observe the expected differences, possibly due to limited measurement accuracy, biological variability and small tissue volumes.[26] Electrical impedance studies assume that the accelerated protein synthesis accompanying remodeling should increase impedance in the cervix. In late gestation, impedance is increased in humans but the technique is not useful for detection of small changes in microstructure.[27]

These and other techniques (x-ray diffraction, electron microscopy and magnetic resonance imaging) have contributed to an emerging model of cervical microstructure, although it is far from complete.[28, 29] In fact, recent studies involving increasingly sophisticated techniques are making the picture murkier; one MRI study found that "a clear scheme of fiber orientation is not immediately recognizable"[30]

Because it appears that the most important contributor to cervical strength in pregnancy is the reorganization and realignment of collagen in response to major biochemical and molecular events that cause cervical change, our goal is to develop a method to objectively and quantitatively assess this component of cervical microstructure noninvasively.

## METHODS

Our methods are aimed at determining whether we can detect the aligned, organized collagen microstructure of the nonpregnant cervix. Ten cervix specimens were obtained from nonpregnant subjects undergoing hysterectomy for benign conditions. We chose nonpregnant, benign specimens because (a) the collagen in the nonpregnant cervix is known to be anisotropic[22] and (b) we wished to avoid confounding due to potential remodeling occurring in inflammatory states (e.g. malignancy).

We estimated the total backscattered power in the specimens because the total backscattered power received by a transducer after an ultrasound beam has been transmitted is a simple measure of the tissue's ability to 'reflect' ultrasound waves and is directly proportional to the acoustic backscatter coefficient – a quantitative measure of acoustic scattering on an absolute scale. This acoustic property can be used to investigate tissue anisotropy by comparing backscattered power as a function of the acoustic beam angle relative to the tissue alignment because waves will scatter differently in tissue that is isotropic compared to anisotropic.

Within one hour of receipt from the operating room, the hysterectomy specimen was placed in a bath of physiologic saline and scanned with a linear array transducer (Siemens SONOLINE Antares VFX9-4; Siemens Healthcare, Inc., Ultrasound Division, Mountain View, CA). The transducer has a center frequency of approximately 7 MHz, approximately 70% fractional bandwidth at –6dB, and is focued in elevation at about 25 mm and 45 mm for the inner and outer apertures of a 1.25D array. The cervix was interrogated longitudinally and transectionally in a circumferential fashion at 12:00, 3:00, 6:00 and 9:00 (Fig. 1). Radio-

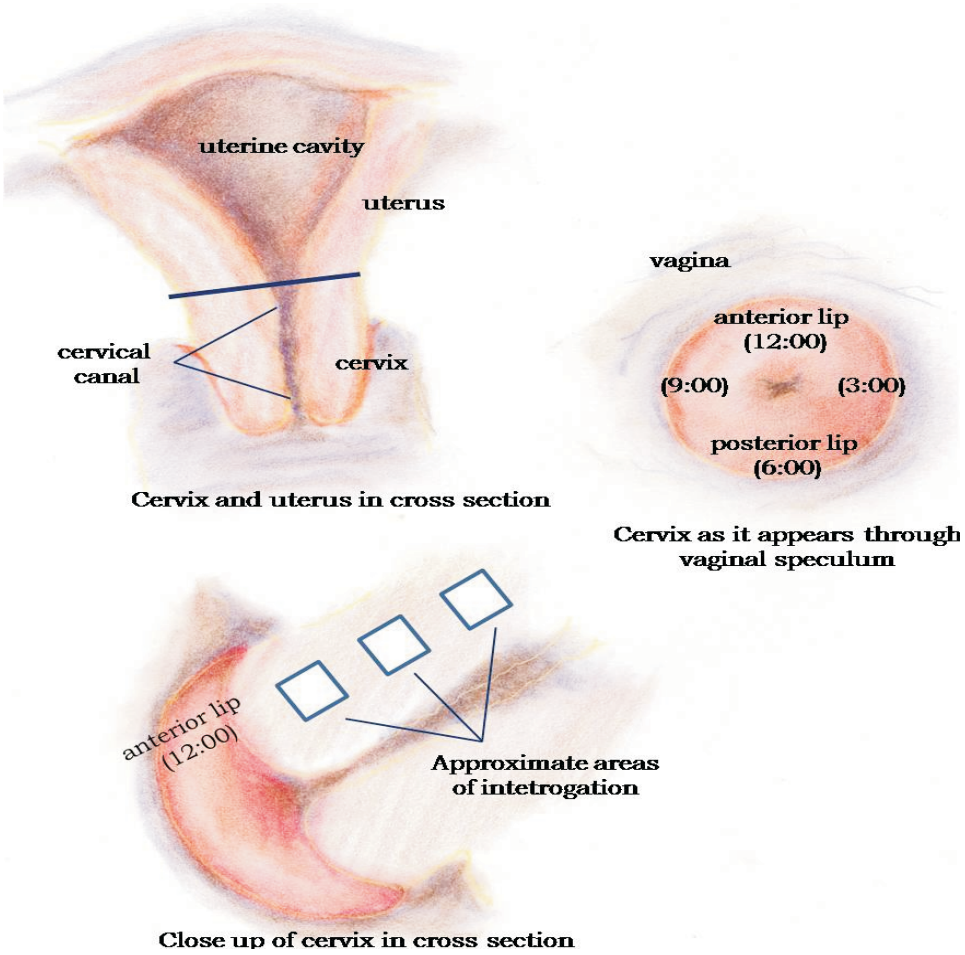


**FIG. 1** Illustration of cervical anatomy, demonstrating from where measurements were obtained

frequency (rf) echo data were acquired with the endocervical canal in the image plane and parallel to the transducer face, as shown in figure 2. At each position, the transducer was held steady and the ultrasound beam electronically steered from -20° to +20° (Fig. 3). The study was approved by the Institutional Review Board at the University of Wisconsin.

From the B-mode image, a region of interest (5 mm × 5 mm) was arbitrarily selected in the center of the field between the cervical canal and the proximal external surface of the cervix (Fig. 3a) and the beam steered from –20° to +20° (in steps of 5°) within it (Figs. 3a-c). The power spectrum of rf echo signals was then computed for each beam steering angle to assess for anisotropy; if an organized and aligned microstructural component (such as collagen) is present, it will likely cause anisotropy in acoustic scattering and thus the backscattered power would be (beam steering) angle-dependent. To assure result consistency and determine whether the scatterer is present throughout the cervix, similar locations (center of the field between the canal and eternal surface) were interrogated along the entire length of the cervix (Fig. 1).

In order to interpret measurements from the cervical tissue, rf data were then acquired in the same manner from an isotropic phantom with spatially randomly-distributed spherical scatterers (spheres look identical from any angle and thus cause beam-steering angle-independent backscattering[31]). Comparison with an isotropic phantom is necessary because of an

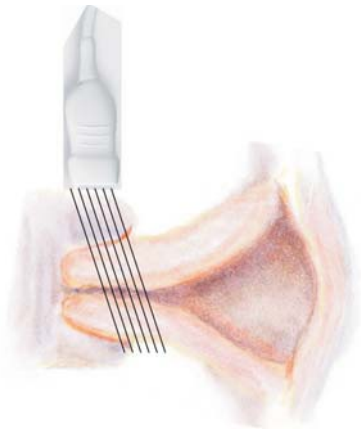

**FIG. 2** Illustration of a linear array acquiring steered beams of rf echo data

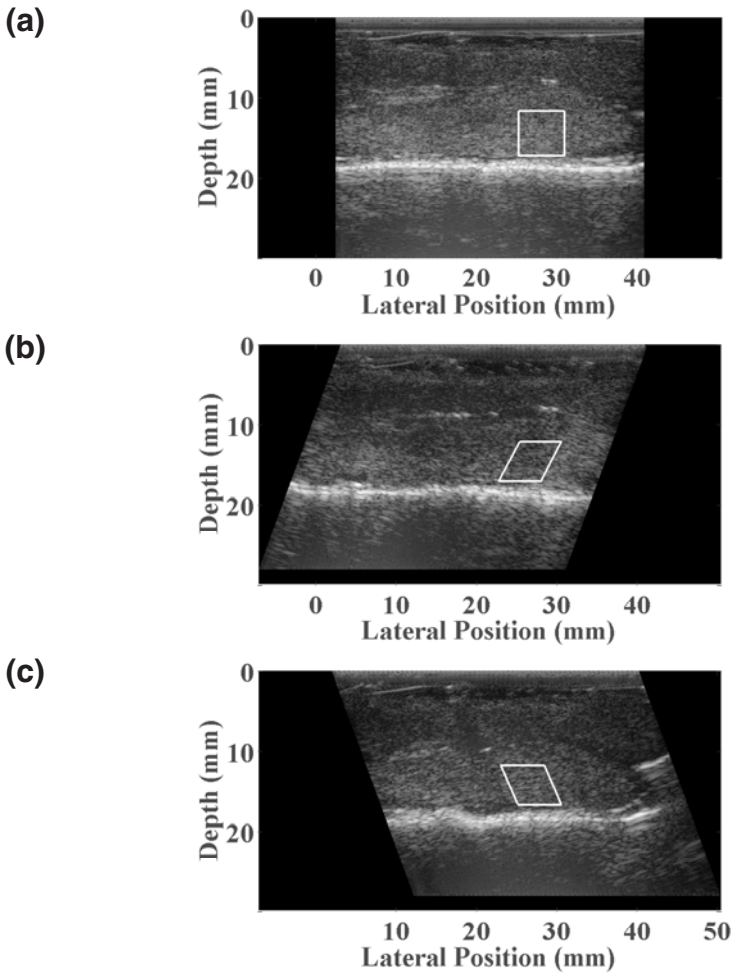


**FIG. 3** (a) B-mode image of cervix specimen showing example of region-of-interest location for beam steering angle of 0°. The echogenic horizontal line is the cervical canal. (b) B-mode image of cervix specimen showing example of region-of-interest location for beam steering angle of –20°. (c) B-mode image of cervix specimen showing example of region of interest location for beam steering angle of +20°.

angle-dependent loss in system sensitivity that is independent of the isotropic or anisotropic nature of the component under investigation and therefore must be taken into account. Specifically, as the steering angle of an ultrasound beam increases, the decrease in effective aperture and sensitivity of the array causes a predictable loss in backscattered power. This loss is a system effect and will occur as an ultrasound beam is steered away from the normal incident angle ($0^{o}$) no matter what material is interrogated. In an isotropic medium, the loss in backscattered power as the steering angle of the beam increases is due exclusively to this system effect.

In contrast, backscatter measurements from anisotropic media are angle-dependent. When a beam encounters an anisotropic medium, there will be excess backscattered power loss in addition to the loss from system effects. This is because the scattering structures in anisotropic media (such as aligned rods) do not appear the same from all angles and the backscattered waves demonstrate that difference. A sound wave that encounters a rod-like cylinder at normal incidence ($0^{o}$) excites only circumferential modes of vibration (which causes backscatter), just as a sound wave that encounters a spherical scatterer. However, a wave that encounters the same cylinder at an angle non-normal to its axis (at either a positive or negative angle) excites both axial and circumferential modes of vibration[32] causing a loss in backscattered power that is increased over that due to the system effect. As a result, the backscattered power and power loss (relative to normal incidence) depends on the angle of incidence relative to the structural alignment of the scatterer encountered; generally, the greater the angle, the greater the power loss. Therefore, comparison of the backscattered power loss in a tissue to that from an isotropic phantom (to account for the system effects) gives information about the tissue's microstructure, specifically with regard to its isotropy/anisotropy.

To investigate the anisotropic properties of the cervical tissue, after scanning both the specimens and the phantom, we objectively quantified and compared the backscattered power measurements by integrating the individual power spectra of the rf echo signals within the region of interest. The limits of integration (the lower and upper frequency cut-off points) were established to assure consistency and immunity from noise among backscattered power estimates. Because the noise floor varies from one data-set to another, the electronic noise floor in the power spectrum was visually established and the frequency range over which the echo signal power exceeded the noise floor by 10 dB was selected for integration.

Further, in order to compare measurements equally, a consistent frequency band was used for all beam steering angles for that data set (a particular cervix specimen and the corresponding phantom data). The most narrow suitable frequency range within a data set was applied to the entire data set for consistency. For example, the frequency range for the integrated backscattered rf power was between about 3 MHz and 9 MHz and this frequency range was used for all data from that cervix and for comparison with the spherical scatterer phantom at all beam steering angles.

To compare backscattered echo signal power at the various acoustic beam steering angles the spectral power was normalized to that at $0^{o}$ using $dB = 20 \log (A/B)$ where $A$ is the power at the specific steering angle under consideration and B is the power at $0^{o}$. In this approach, lower echo signal power is expressed as a loss compared to $0^{o}$ steering angle backscattered power.

The backscattered echo signal power spectra were also normalized to the peak of the power spectrum to investigate whether noted losses in backscattered power suggested presence of an anisotropic scattering structure or, instead, could be attributed to frequency-dependent differences in scattering or attenuation. In other words, our aim was to determine whether there was a change in the shape of the power spectrum (frequency-dependent changes such as those due to attenuation or scattering) rather than a total (frequency-inde-

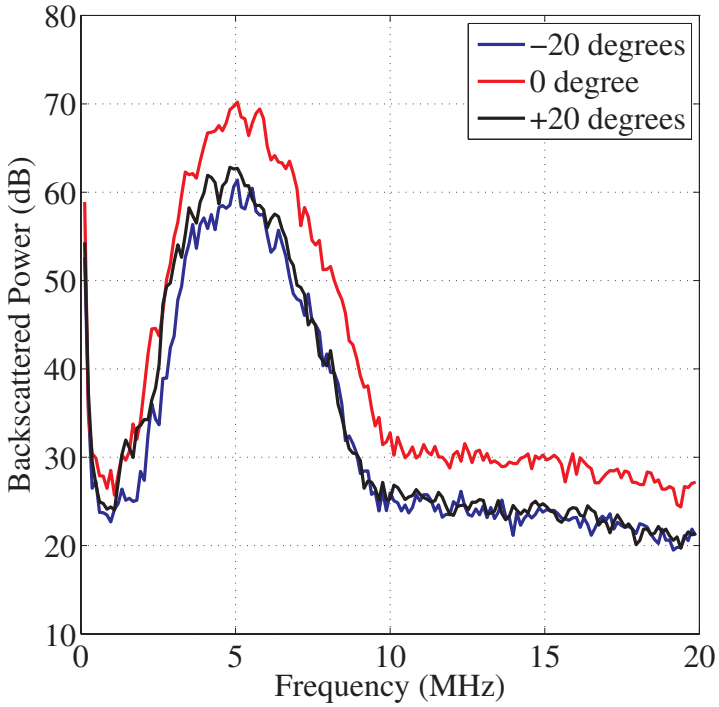


**FIG. 4** Backscattered echo signal power spectra from a cervix at three beam-steered angles (–20°, 0°, +20°) for 6 MHz pulsing frequency.

pendent) loss of scattered power (such as due to beam interaction with an anisotropic scatterer). For instance, in the case of total loss of power, a uniformly-downshifting spectrum is expected, however, frequency-dependent changes are not be expected to be uniform. If a change in the attenuation coefficient with beam steering angle were the cause of the loss in spectral power, one would expect a larger difference on the high frequency side of the spectral curve because of the increase in attenuation at higher frequencies. The resulting change in power spectral shape due to a change in the effective scatterer size is difficult to predict, but it is unlikely to be a frequency-independent loss. Given these varied expectations, it seemed most efficient and logical to use visual inspection of the curve to determine whether our findings were due to frequency-dependent phenomena or detection of an anisotropic component of the cervical microstructure.

A student's t-test was used to compare backscattered power loss from the isotropic phantom to the average value from the 10 cervical specimens to determine whether there was a significant difference in backscattered power as a function of beam steering.

These measurements were performed at 6 MHz and 9 MHz transmit frequencies to verify robust and predictable estimates of backscattered power and to determine if measurements demonstrated any frequency dependence. We adjusted the bandwidth for analysis of each of the datasets (each cervix) as well as for each pulse frequency.

## RESULTS

The backscattered power as a function of beam steering angle for a particular sample (either cervix specimen or phantom) was compared to data from that particular sample at 0°

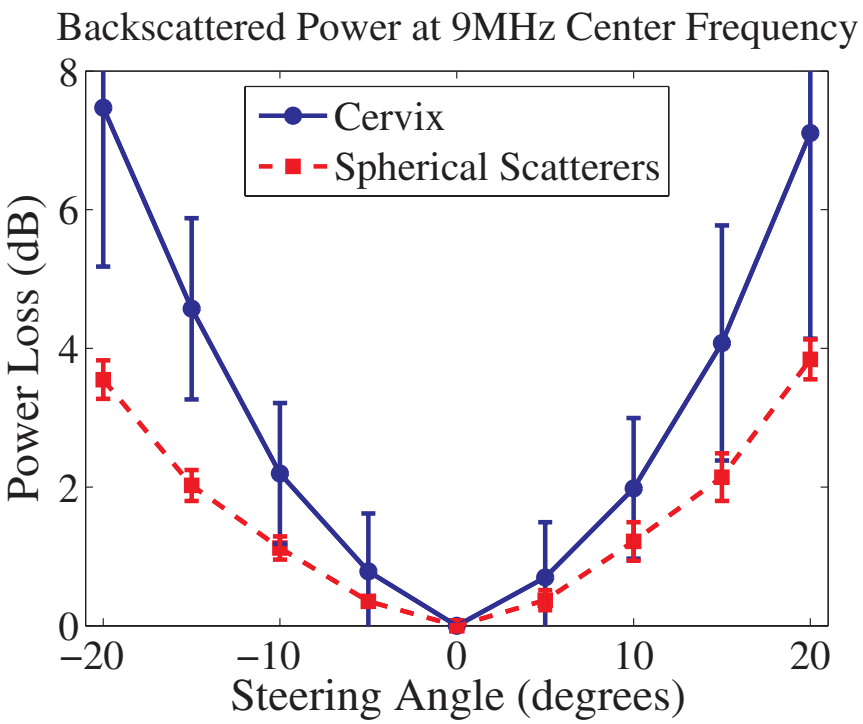


**FIG. 5** Backscattered echo signal power as a function of acoustic beam steering angle normalized to that at 0° angle. Note that the power loss is symmetric about 0° and monotonically increases with increased steering angle.

(acoustic beams normal to the transducer face) to address differences in absolute backscattered power among specimens. As discussed in the Methods section, comparison with an isotropic phantom is necessary because there is angle-dependent loss in system sensitivity that is independent of the properties of the material under investigation. An example of this comparison is shown in figure 5. The figure shows symmetry in the average backscattered power loss about the 0° beam steering angle, as expected for an organized, aligned scattering structure because the magnitude of the angle (not whether it is positive or negative) should determine the backscatter. Demonstration of symmetry made it possible to average results of equivalent magnitude beam steering angles (e.g. −5° and +5°) in order to reduce variance in estimates of backscatter power loss. After doing this, we found that loss of backscattered power monotonically increases as a function of steering angle in cervical tissue and in the phantom (Fig. 6). We also found that the backscattered power loss at equivalent angles was larger at a 9 MHz pulse center frequency than at 6 MHz, all else being equal (Fig. 7).

One possible confounding factor in determining the excess backscattered power loss in the cervix, compared to spherical scatterers in the phantom, is that there might be a change in the shape of the power spectra (for example, due to a change in the frequency dependence of scattering from a change in effective scatterer size) as the acoustic beam is steered. Therefore, we normalized the backscattered power spectra to their peak value and compared the normalized spectra among steering angles so that we could visually analyze differences in the frequency content of the spectra. After normalization, the backscattered echo signal power spectra were nearly identical (Fig. 8). This strongly suggests that there are no significant differences in the effective size of the scattering source as the acoustic beam angle changes (from 0° to 20°). The analysis also eliminates changes in the mechanism for acoustic attenuation of the wave as another potential source for the excess power loss.

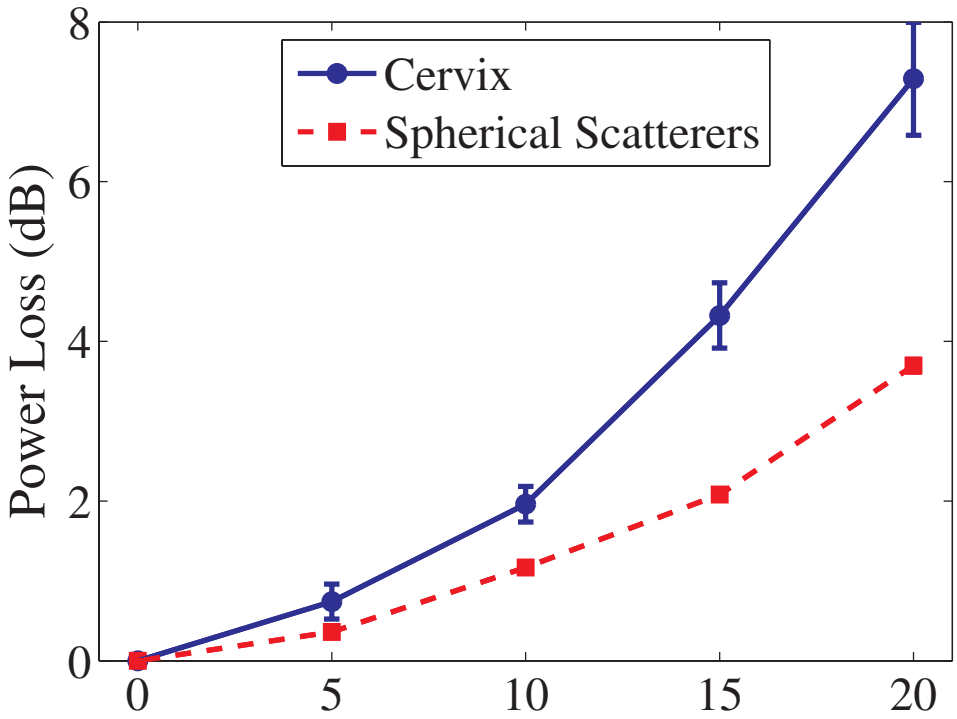


**FIG. 6** Backscattered echo signal power as a function of acoustic beam steering angle normalized to that at 0° angle after combining results at equivalent magnitude angles.

Finally, similar results were obtained throughout the region centered between the cervical serosa and the cervical canal and at all positions along the cervical length, suggesting that the component of the cervical microstructure we are detecting is ubiquitous in the cervix.

## DISCUSSION

Our results suggest scattering from an anisotropic component in the cervical tissue that is aligned with the cervical canal because: (a) excess backscattered echo signal power loss is symmetric about 0° steering angle (Fig. 5), (b) excess power loss increases monotonically with increased steering angle magnitude (Fig. 6), (c) normalized backscattered echo signal power spectra are nearly identical at all angles for a given cervix (Fig. 8) and (d) power loss is (pulse) frequency-dependent (Fig. 7). Taken together, these results implicate collagen, the most ubiquitous component of the cervical microstructure and which is known to behave anisotropically in the nonpregnant cervix.

In summary, despite many studies that attest to the importance of clarifying and understanding cervical microstructure, currently, there are no objective, reliable and quantitative methods to interrogate collagen in the cervix; thus, the cervix remains a mystery. Objective exploration of this mystery through accurate assessment of cervical microstructure is promising. One investigator said that "ultrasound cannot measure biochemical parameters of cervical ripening, nor can it provide direct histological information about connective tissue structure."[20] While this is strictly true, our preliminary study of quantitative ultrasound suggests that cervical microstructure changes can be quantified and accurately described.

Although our results are encouraging, we have not yet confirmed that we are detecting collagen. To corroborate our ultrasound findings, we are currently using nonlinear optical mi-

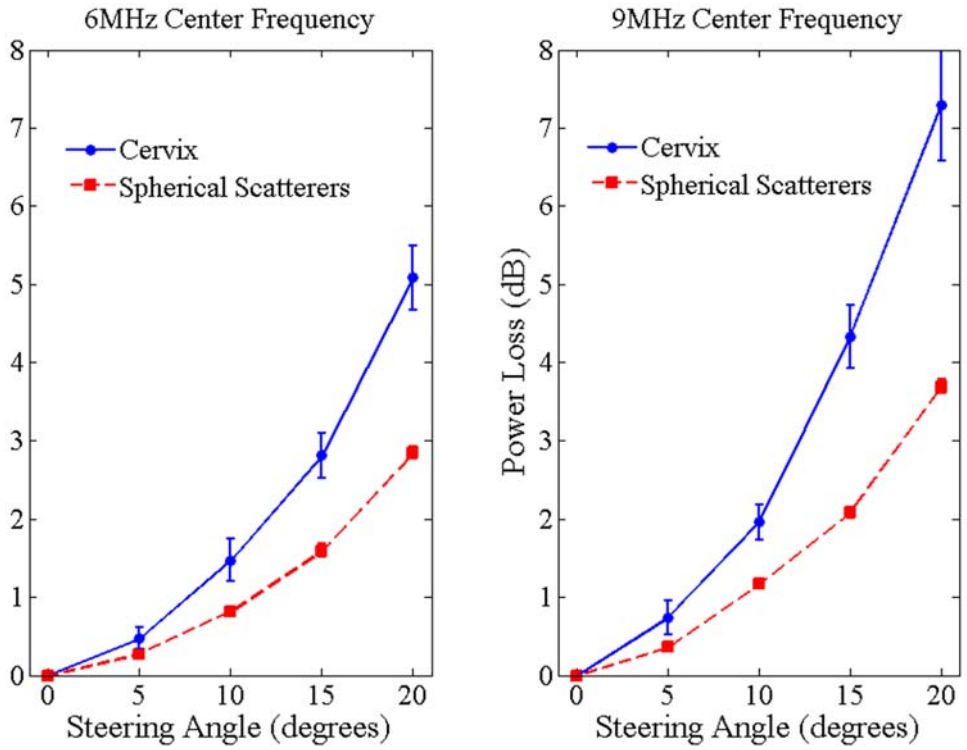


**FIG. 7** Backscattered echo signal power as a function of acoustic beam steering angle normalized to that at 0° angle comparing results for 6 MHz pulses versus 9 MHz pulses.

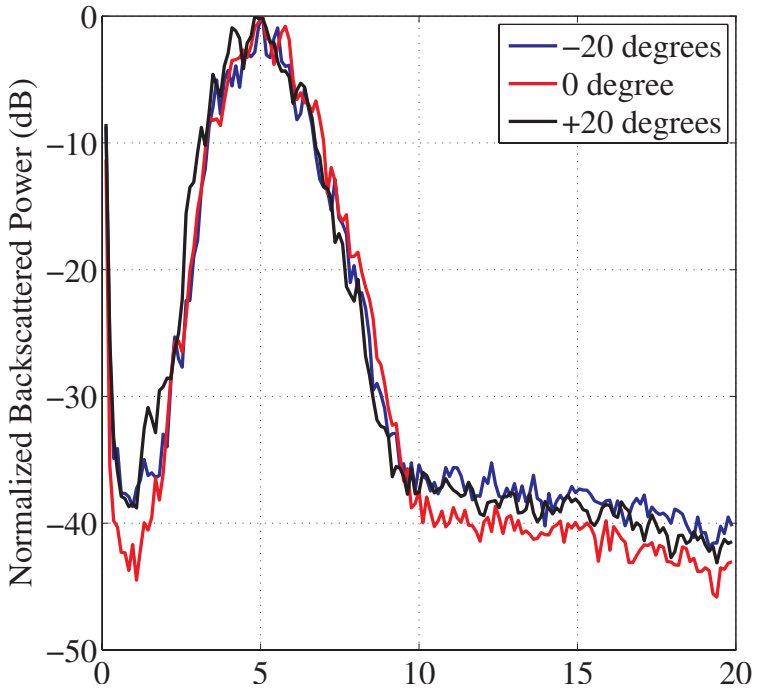


**FIG. 8** Normalized backscattered echo signal power spectra from the cervix at three beam-steered angles showing nearly identical shapes for 6 MHz pulsing frequency.

croscopy to image the collagen microstructure and objectively quantifying collagen orientation. Further, we are investigating whether the remodeled cervix demonstrates different backscattered power loss than the unremodeled cervix. Because cervical collagen increasingly disorganizes as gestation progresses, it should become more isotropic. The ability to measure this could give a remarkable new insight into the process of cervical microstructural change throughout pregnancy. Ultimately, a comprehensive understanding of cervical remodeling could provide information about early changes that occur prior to irreversible gross changes, thus opening pathways to novel approaches to prediction and prevention of preterm birth.

## REFERENCES

1. Spong CY. Prediction and prevention of recurrent spontaneous preterm birth, *Obstet Gynecol 110,* 405-415 (2007).

2. Goldenberg RL, Culhane JF, Iams JD, Romero R. Preterm birth 1-epidemiology and causes of preterm birth, *Lancet 371,* 75-84 (2008).

3. Romero R, Espinoza J, Erez O, Hassan S. The role of cervical cerclage in obstetric practice: can the patient who could benefit from this procedure be identified, *Am J Obstet Gynecol 194,* 1-9 (2006).

4. Coomarasamy A, Thangaratinam S, Gee H, KS K. Progesterone for the prevention of preterm birth: a crucial evaluation of evidence, *Eur J Obstet Gynecol Reprod Biol 129*, 111-118 (2006).

5. Fonseca EB, Celik E, Parra M, Singh M, Nicolaides KH. Progesterone and the risk of preterm birth among women with a short cervix, *New Engl J Med 357,* 462-469 (2006).

6. Defranco E, Obrien J, Adair C. Vaginal progesterone is associated with a decrease in risk for early preterm birth and improved neonatal outcome in women with a short cervix: a secondary analysis from a randomized, double-blind, placebo-controlled trial, *Ultrasound Obstet Gynecol 30*, 697-705 (2007).

7. Xu H, Gonazalez JM, Ofori E, Elovitz MA. Preventing cervical ripening: the primary mechanism by which progestational agents prevent preterm birth, *Am J Obstet Gynecol 198,* 314.e1 (2008).

8. Meis P. 17 hydroxyprogesterone for the prevention of preterm delivery, *Obstet Gynecol 105,* 1128-1135 (2005).

9. Goldenberg R (NICHD Maternal-Fetal Medicine Unit Network). The preterm prediction study: sequential cervical length and fetal fibronectin testing for the prediction of spontaneous preterm birth, *Am J Obstet Gynecol 182,* 636-6543 (2000).

10. ACOG, Assessment of risk factors for preterm birth, *American College of Obstetricians and Gynecologists., Bulletin #31*(2006).

11. Maul H., Mackay L, Garfield RE. Cervical ripening: biochemical, molecular, and clinical considerations, *Clin Obstet Gynecol 49,* 551-563 (2006).

12. Winkler M, Rath W. Changes in the cervical extracellular matrix during pregnancy and parturition*, J Perinat Med 27,* 45-60 (1999).

13. Leppert P. Anatomy and physiology of cervical ripening, *Clin Obstet Gynecol 38(2)*: 267-279 (1995).

14. Danforth D, The morphology of the human cervix, *Clin Obstet Gynecol 26,* 7-13 (1983).

15. Rechberger T, Abramson SR, Woessner JF. Onapristone and prostaglandin E2 induction of delivery in the rat in late pregnancy: a model for analysis of cervical softening, Am J Obstet Gynecol 175, *719-723 (1996).*

16. Word RA, Li XH, Hnat M, Carrick K. Dynamics of cervical remodeling during pregnancy and parturition: mechanisms and current concepts, *Sem Reprod Med 25,* 69-79 (2007).

17. Fittkow C, Maul H, Olson G, et al. Light-induced fluorescence of the human cervix decreases after prostaglandin application for induction of labor at term, *Eur J Obstet Gynecol Reprod Biol 123*, 62-66 (2005).

18. Mahendroo M, Porter A, Russell D, Word R. The parturition defect in steroid 5-alpha-reductase type 1 knockout mice is due to impaired cervical ripening, *Mol Endocrinol 13,* 981-992 (1999).

19. Bishop E. Pelvic scoring for elective induction, *Obstet Gynecol 24*, 266-269 (1964).

20. Yu S, Tozzi C, Babiarz J, Leppert P. Collagen changes in rat cervix in pregnancy – polarized light microscopic and electronic microscopic studies, *Proc Soc Exp Biol Med 209*, 360-368 (1995).

21. Feltovich H, Janowski J, Carroll C, Chien E. The effects of nonselective and selective PGE2 receptor agonists on cervical tensile strength and cervical collagen content and structure, *Am J Obstet Gynecol 9,* 753-760 (1995).

22. Myers KM, Socrate S, Paskaleva A, House M. A study of the anisotropy and tension/compression behavior of human cervical tissue, *J Biochem Eng 132,* (2010).

23. Tekesin I, Wallwiener D, Schmidt S. The value of quantitative ultrasound tissue characterization of the cervix and rapid fetal fibronectin in predicting preterm delivery, *J Perinat Med 33, 3*83-391 (2005).

24. Jorn H, Kalf K, Schwann R, Rath W. Grey-scale texture analysis of the cervix in pregnancy, *Ultraschall in Der Medizin 27,* 347-354 (2006).

25. Maul R, Saade G, Garfield R. Prediction of term and preterm parturition and treatment monitoring by measurement of cervical cross-linked collagen using light-induced fluorescence, *Acta Obstetricia Et Gynecol Scand 84,* 534-536 (2005).

26. Bigelow T, McFarlin B, O'Brien WD, Oelze ML. In vivo ultrasonic attenuation slope estimates for detecting cervical ripening in rats: preliminary results*, J of Acoustical Society America 123,* 1794-1800 (2008).

27. Gandhi S, Walker D, Milnes P, et al. Electrical impedence spectroscopy of the cervix in non-pregnant and pregnant women, *Eur J Obstet Gynecol Reprod Biol 129,* 145-149 (2006).

28. Mazza E, Nava A, Bauer M, et al. Mechanical properties of the human uterine cervix: an in vivo study, *Med Image Anal 10,* 125-136 (2006).

29. Thomas A, Kummel S, Gemeinhardt O, Fischer T. Real-time sonoelastography of the cervix: tissue elasticity of the normal and abnormal cervix, *Acad Radiol 14,* 193-200 (2007).

30. Weiss S, Jaermann T, Schmid P, et al. Three-dimensional fiber architecture of the nonpregnant human uterus determined ex vivo using magnetic resonance diffusion tensor imaging, *Anatomical Record Part A 288A*, 84-90 (2006).

31. Faran JJ. Sound scattering by solid cylinders and spheres, *J Acoust Soc Amer 23,* 405-418 (1953).

32. Flax L, Varadan VK, Varadan VV. Scattering of an obliquely incident acoustic-wave by an infinite cylinder, *J Acoust Soc Amer 68,* 1832-1835 (1980).